Modelling the creep behaviour of HMPE fibers used in ultra-deep-sea mooring ropes

H.S. da Costa-Mattos
LMTA – Laboratório de Mecânica Teórica e Aplicada, Departamento de Engenharia Mecânica, Universidade Federal Fluminense, Niterói/RJ – Brazil
F.E.G. Chimisso
POLICAB – Laboratório de Análise de Tensões, Escola de Engenharia, Fundação Universidade Federal do Rio Grande, Rio Grande/RG – Brazil

Abstract

Due to its low density and high strength, HMPE (high modulus polyethylene) fibres are increasingly used in synthetic ropes for offshore mooring. Nevertheless, the occurrence of significant creep deformation at sea temperature is a major shortcoming for its practical use. The present paper is concerned with a methodology to predict creep lifetime of HMPE yarns in this macroscopic approach, besides the classical variables (stress, total strain), an additional scalar variable related with the damage induced by creep is introduced. An evolution law is proposed for this damage variable. The main goal is to present model equations that combine enough mathematical simplicity to allow their usage in engineering problems with the capability of describing a complex non-linear mechanical behaviour. The model prediction is compared with curves obtained experimentally at room temperature showing a good agreement.

Keywords: synthetic mooring ropes, continuum damage mechanics, creep, lifetime prediction.

1 Introduction

With the development of oil fields in ultra deep waters, the replacement of steel ropes used to mooring floating structures by other with lesser linear weight, become a necessity. In shallow waters the drilling and production flotation units are anchored by conventional systems composed of steel chains and wire ropes in catenary geometric configurations. For deep and ultra deep waters the "taut-leg" [1, 2] system based on tightened synthetic ropes with lesser linear weight was developed. Nowadays these ropes provide the necessary compliance to the taut-leg system by means of the natural mechanical properties of the fibres.

Most fibre ropes comprise a core to withstand tensile loads and an outer jacket, which often has

Mechanics of Solids in Brazil 2009, H.S. da Costa Mattos & Marcílio Alves (Editors)
Brazilian Society of Mechanical Sciences and Engineering, ISBN 978-85-85769-43-7

little tensile load bearing capability. Additional protective coatings or wrappings may be applied after rope manufacture. Typical rope construction types suitable for deepwater fibre moorings are wire rope constructions (WRC), and parallel strand types. The main structural levels in a fibre rope, although not all present in every construction, are: (i) Textile yarns, as made by the fibre producer and typically consisting of hundreds of individual filaments; (ii) Rope yarns, assembled from a number of textile yarns by the rope maker; (iii) Strands made up from many rope yarns; (iii) Sub-ropes of several strands; (v) The complete core rope assembly; (v) Rope, sub-rope and strand jackets.

Polymer based fibre ropes exhibit nonlinear behaviour and are subject to creep, potentially leading to creep rupture. Polyester ropes are not subject to significant creep at loads normally experienced in mooring applications. HMPE - High Modulus Polyethylene is a material with excellent mechanical behaviour in tension and lower density than polyester, but with significant creep at normal conditions of temperature. HMPE yarns creep substantially, although the rate of creep is very dependent on the particular HMPE yarn in question.

The analysis of creep phenomenon in HMPE synthetic ropes accounting for different rope constructions can be extremely complex. The mechanisms proposed so far to explain the damage initiation and propagation processes are not able to elucidate all aspects of the phenomenon in different geometry/material systems [3–9]. Despite the lack of definition of a basic theory for creep failure for such complex systems, the evaluation of the susceptibility to creep is a basic requirement for safe and economic operation, since creep rupture remains as one of the main limitations for the use of HMPE synthetic ropes for deep water mooring of FSOP units and floating platforms. This objective is accomplished by the execution of a set of laboratory tests taking as specimen a sub-system (yarn). Creep tests in textile yarns, as made by the fibre producer and typically consisting of hundreds of individual filaments, are frequently used in order to obtain more detailed information about the macroscopic creep behaviour of the fibres. These tests are so far the most important techniques used to rank the susceptibility of different materials in a specific temperature. However, it is necessary a large number of tests in order to provide basic parameters to be directly used in engineering design, mainly to estimate the influence of the load and temperature on the creep process. Hence, the determination of the creep behaviour of HPE yarns is up to now strongly dependent on these CL tests, what makes attempts to model these tests advisable.

The present paper is concerned with the phenomenological modelling of creep tests of HMPE yarns at room temperature. The goal is to propose a one-dimensional phenomenological elasto-viscoplastic model that combines enough mathematical simplicity to allow its usage in engineering problems with the capability of describing a complex non-linear mechanical behaviour. The main idea is to use such model to obtain the maximum information in order to rank the susceptibility of different materials to creep from a minimum set of laboratory tests, saving time and reducing experimental costs.

In this phenomenological approach, besides the classical variables for an isotropic elasto-viscoplastic material (stress, total strain, plastic strain), the basic idea is to introduce an auxiliary macroscopic variable $D \in [0, 1]$, related to the loss of stiffness of the specimen due to the damage (geometrical discontinuities induced by mechanical deformation and the simultaneous corrosion processes. If $D = 0$, the specimen is considered "virgin" and if $D = 1$, it is "broken" (it can no longer resist to mechanical loading). An evolution law is proposed for this damage variable. Examples are presented in order to

Mechanics of Solids in Brazil 2009, H.S. da Costa Mattos & Marcílio Alves (Editors)
Brazilian Society of Mechanical Sciences and Engineering, ISBN 978-85-85769-43-7

illustrate the main features of the model.

2 Material and experimental procedures

Long term creep tests were performed in multi-filaments of HMPE using an electromechanical test machine with special clamps for yarn tests in an atmosphere controlled room, with the following environmental conditions: 55 ± 2% of humidity and 20 ± 2 °C of temperature.

The HMPE fibre is produced from the ultra high molecular weight polyethylene (UHMW-PE) by the gelspinning process. In this process the molecules of UHMW-PE fibre are dissolved in a solvent. The obtained solution is successively pulled through small holes and afterwards solidified by cooling it. This process produces a fibre with a chemical structure composed by chains with a high molecular orientation degree (over 95%), as shown in Fig. 1. This molecular structure, with high crystalline degree (up to 85%) and a little amorphous content, gives the fibre a high modulus and a high rupture load.

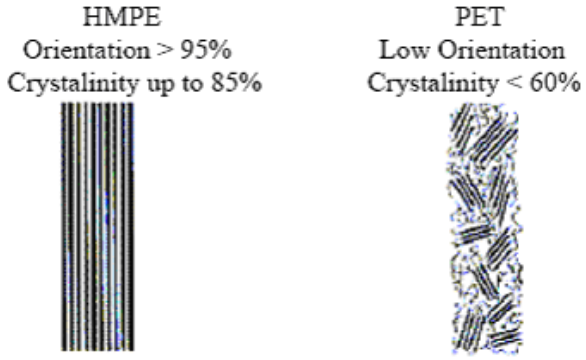

Figure 1: Orientation and Cristalinity representation of HMPE and Polyethylene fibres.

The stress σ at a given instant t can be defined as the rate between the applied tensile force $F(t)$ and the average yarn fibre area A_o

$$\sigma(t) = \frac{F(t)}{A_o} \; ; \; A_o = \frac{\rho_l}{\rho} \Rightarrow \sigma(t) = F(t)\left(\frac{\rho}{\rho_l}\right) \tag{1}$$

where ρ_l is the mass of fibre per unit length and ρ the mass density of fibre material. Since the mass density ρ is the same for a given polymer material, to define the stress of a general yarn regardless the number of fibres it is only necessary to consider the tensile force F divided by the mass of fibre per unit length ρ_l:

$$\hat{\sigma}(t) = \frac{\sigma(t)}{\rho} = \frac{F}{\rho_l} \tag{2}$$

The HMPE multi-filaments tested in this work have linear weight $\rho_l = 1760$ dtex (where 1 dtex = 1 g /10000m). dtex is the most used unit for linear density of a yarn in textile industry and hence it will be adopted on the present study. Each specimen with initial length $L_o = 500 \pm 1$mm was initially loaded at a rate $\alpha = 8{,}3$ N/sec until a limit constant load F_o. Fig. 2 shows the typical loading history the specimens are submitted to.

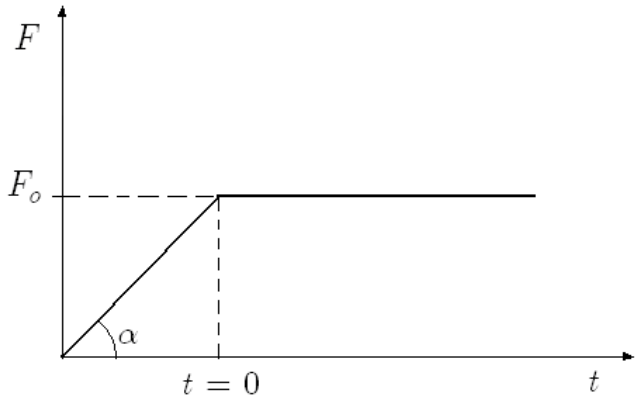

Figure 2: Typical loading history in a long term creep test.

The strain ε at a given instant t can be defined as the rate between the elongation $\delta(t)$ and the initial length L_o

$$\varepsilon(t) = \frac{\delta(t)}{L_o} \tag{3}$$

3 Results and discussion

3.1 Creep testing – Elongation curves at different load levels

Fig. 3 shows experimental creep curves at different load levels (level 1: $F_o = 86{,}3$ N; level 2: $F_o = 172{,}6$ N; level 3: $F_o = 345{,}3$ N; level 4: $F_o = 374$ N; level 5: $F_o = 402{,}7$ N; level 6: $F_o = 431{,}5$ N). The rupture force in a tensile test with prescribed load history $F(t) = \alpha t$ is dependent of the rate α. For a rate $\alpha = 8{,}3$ N/sec, the average rupture force (F_r/ρ_l) is 573,3 N (hence the rupture stress $\hat{\sigma}_r$ for any multi-filament of this particular HMPE is given by $(F_r/\rho_l) = 575{,}3/1760 \approx 0{,}33$ N/dtex). The load levels correspond, respectively, to 15%, 30%, 60%, 65%, 70% and 75% of the rupture force.

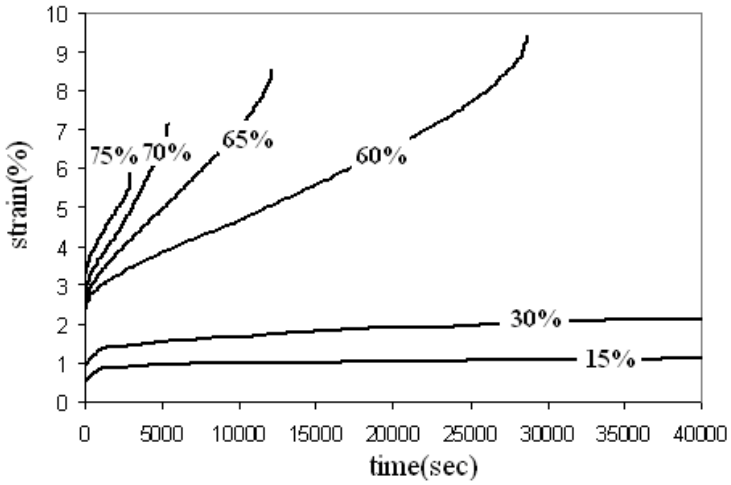

Figure 3: Experimental creep curves at different load levels.

From Fig. 3, it is possible to observe that a typical experimental curve shows three phases of behaviour: (i) a "primary" creep phase during which hardening of the material leads to a decrease in the rate of flow which is initially very high; (ii) a "secondary" creep phase during which the rate of flow is almost constant; (iii) a "tertiary" creep phase during which the strain rate increases up to fracture (see Fig. 4).

It can be verified that the load level strongly affects the creep deformation rate and creep lifetime. Table 1 presents the experimental lifetimes obtained for different load levels. The secondary creep rates ($\dot{\varepsilon}^s$) for different load levels are depicted in Table 2.

Table 1: Experimental creep lifetimes for different load levels. α = 8,3 N/sec.

F_o **(N)**	t_r **(sec)**
345,3	28.710
374,0	12.162
402,7	5.425
431,5	2.935

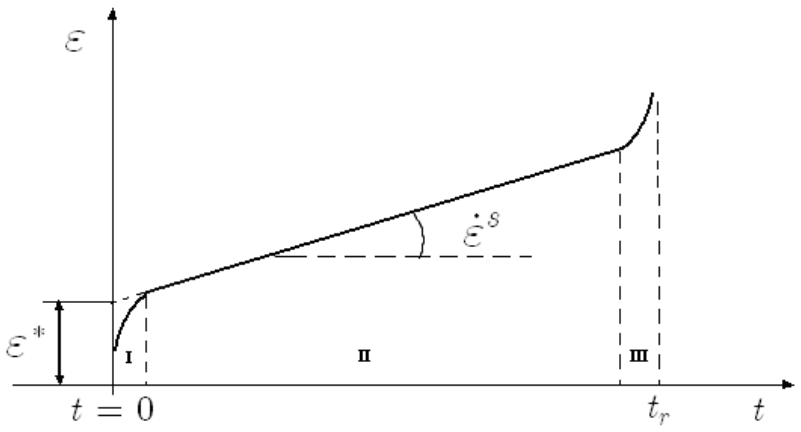

Figure 4: Typical experimental creep curve.

Table 2: Experimental secondary creep rate for different load levels. α = 8,3 N/sec.

F_o **(N)**	$(\dot{\varepsilon}^s)$ **(% sec^{-1})**
86,3	0,0000014
172,6	0,000094
345,3	0,00017
374,0	0,00039
402,7	0,00058
431,5	0,00074

The strain $\varepsilon*$ (Table 3) is related to the secondary creep and depends on the loading rate α and of the maximum force level F_o.

3.2 Modelling

In this paper, in order to provide a better understanding of the results from creep tests, a simple one-dimensional model is proposed. The main goal is to present model equations that combine enough mathematical simplicity to allow their usage in engineering problems with the capability of describing a complex non-linear mechanical behaviour. All the proposed equations can be developed from ther-

Table 3: Experimental values of $\varepsilon*$ for different load levels. α = 8,3 N/sec.

F_o **(N)**	$\varepsilon*$ **(%)**
86,3	0,50 1,02
172,6	0,68 1,73
345,3	0,70 2,79
374,0	0,78 3,05
402,7	0,74 3,18
431,5	0,75 3,37

modynamic arguments similar to Sampaio et al [10] and Costa-Mattos [11], that will not be discussed on this paper.

In order to build the model, it is considered as a system a tension specimen with gauge length L_o and a mass of fibre per unit length ρ_l submitted to a prescribed elongation $\delta(t)$. The following model is proposed to describe the creep damage behaviour of HMPE multi filaments:

$$F_o = (1 - D)\, \rho_l E\, (\varepsilon - \varepsilon_v) \tag{4}$$

$$\frac{d\varepsilon_v}{dt} = K\left[\exp(\tfrac{NF_o}{\rho_l}) - 1)\right] \tag{5}$$

$$\frac{dD}{dt} = \left(\frac{SF_o}{\rho_l(1-D)}\right)^R \tag{6}$$

where the variables ε, ε_v are defined as follows

$$\varepsilon = (\delta/L_o);\ \varepsilon_v = (\delta_v/L_o);\ \delta = \delta_e + \delta_v \tag{7}$$

with δ_e being the elastic or reversible part of δ and δ_v the irreversible parcel of δ. The basic idea is to introduce a macroscopic variable $D \in [0, 1]$, related to the loss of stiffness of the specimen due to creep damage. If $D = 0$, the specimen is considered "virgin" and if $D = 1$, it can no longer resist to mechanical loading. E, K, N, S, R, a, b are material constants which depend on the material. Eq. (4) will be called the state law and Eqs. (5), (6) the evolution laws.

Using boundary condition $D\,(t = 0) = 0$, it is possible to find the analytical solution of differential equation (6) that governs the damage evolution in a constant load (creep) test:

$$D(t) = 1 - \left[1 - \left(t\,(R+1)\left(\frac{SF_o}{\rho_l}\right)^R\right)\right]^{\frac{1}{R+1}} \tag{8}$$

Since rupture occurs when $D = 1$, it is possible to compute the time t_r until the rupture

$$D = 1 - \left(1 - \frac{t}{t_r}\right)^{\frac{1}{(R+1)}} \tag{9}$$

From the equations here proposed it is possible to observe that during the creep test the damage variable increases slowly until almost the end of the test ($t = t_r$) when it increases very fast until rupture($D = 1$), as it is shown in Fig.5.

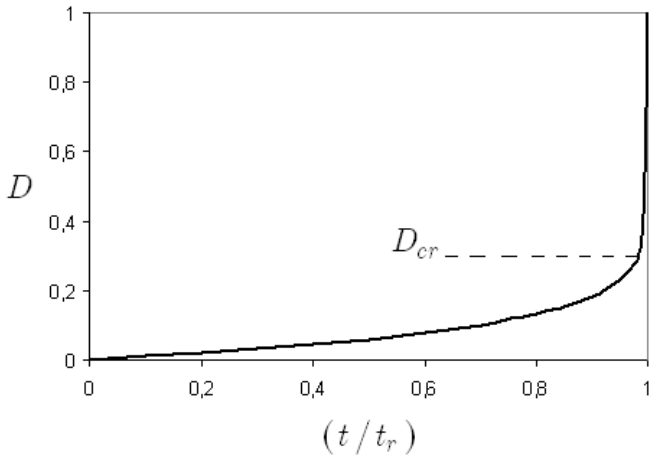

Figure 5: Damage evolution in a typical creep test.

If this kind of damage behaviour is observed, it is usual to consider a critical value D_{cr} of the damage variable, beyond which the evolution to the value toward $D = 1$ is so fast that it can be considered instantaneous. If, in a conservative approach, the failure is considered to occur when $D = D_{cr}$, the following expression is obtained

$$D = 1 - \left[1 - \left(\frac{t}{t_{cr} + \frac{(1+D_{cr})^{R+1}}{R+1}\left(\frac{SF_o}{\rho_l}\right)^{-R}}\right)\right]^{\frac{1}{R+1}} \tag{10}$$

with $t_{cr} = \frac{1-(1-D_{cr})^{R+1}}{R+1}\left(\frac{SF_o}{\rho_l}\right)^{-R}$

From Eq. (9) or (10), the curves of the damage evolution for creep tests under different conditions may be obtained. Examples of these curves are shown in the next section. As it is shown in the next section, the secondary and tertiary stages of the creep curve are fully described by this model. In this model, important parameters, such as steady state elongation rate, and time to failure are also taken into account.

The variables R and S can be identified experimentally from the lifetimes obtained in two creep tests at different load levels, since the behaviour of the $\log(t_r) \times \log(\sigma_0)$ curve is linear, as shown in Eq. (11)

$$t_r = \frac{1}{R+1}\left(\frac{SF_o}{\rho_l}\right)^{-R} = \underbrace{\left(\left(\frac{S}{\rho_l}\right)^{-R}\frac{1}{R+1}\right)}_{\alpha}(F_o)^{-R} \Rightarrow$$

$$\log(t_r) = \log(\alpha) - R\ \log(F_o) \tag{11}$$

Parameters K and N can be obtained from the secondary creep rate ($\dot{\varepsilon}^s$). Supposing that damage is negligible at secondary creep ($D \approx 0$) and that $\frac{d\varepsilon_v}{dt} \approx \frac{d\varepsilon}{dt} = \dot{\varepsilon}^s$ it is possible to obtain

$$\dot{\varepsilon}^s \approx\ K\left[\exp(\tfrac{NF_o}{\rho_l}) - 1)\right] \quad \text{at secondary creep} \tag{12}$$

K and N ca be identified using a minimum square technique. Nevertheless, for practical purposes, it is suggested to initially consider the law $\dot{\varepsilon}^s = \hat{K}\exp\left(\frac{\hat{N}F_o}{\rho_l}\right)$. $\hat{K}$ and $\hat{N}$ can be identified experimentally from the secondary creep strain rates obtained in two tests at different load levels, since the behaviour of the $\log(\dot{\varepsilon}^s) \times F_o$ curve is linear, as shown in Eq. (13)

$$\ln(\dot{\varepsilon}^s) =\ \ln(\hat{K}) + \left(\frac{\hat{N}}{\rho_l}\right)F_o \tag{13}$$

K and N are very close to $\hat{K}$ and $\hat{N}$, and can be approximated (from $\hat{K}$ and $\hat{N}$) using the following iterative procedure:

(a) $i = 0$
(b) $N^i = \hat{N};\ K^i = \hat{K}$;
(c) Compute K^{i+1} from $\ln(\dot{\varepsilon}^s) =\ \ln(K^{i+1}) + \ln\left[\exp(\frac{N^iF_o}{\rho_l}) - 1)\right]$
(d) Once K^{i+1} is known, compute N^{i+1} using $\ln(\dot{\varepsilon}^s) =\ \ln(K^{i+1}) + \ln\left[\exp(\frac{N^{i+1}F_o}{\rho_l}) - 1)\right]$
(e) $i = i + 1$
(f) If $i < i_{\max}$ go to (c). Else $K = K^{i+1}$ and $N = N^{i+1}$

$i_{\max}$ is the maximum allowed number of interactions (suggestion: $i_{\max} = 5$). More sophisticated convergence criteria can be adopted, but they will not be discussed on this paper.

The strain $\varepsilon*$ at instant $t = 0$ is supposed to be given by the following relation (Eq. 5)

$$\varepsilon* = \underbrace{\frac{F_o}{\rho_l E}}_{elasticity} + \underbrace{\left(\frac{a}{\rho_l}\right)^b (F_o)^b}_{primary\ creep} \tag{14}$$

The first parcel is the elastic deformation the second corresponds to the inelastic deformation after primary creep. Parameters a and b can be obtained from two creep tests at different load levels, since the behaviour of the $\log(\varepsilon*) \times \log(F_o)$ is linear, as shown in Eq. (15)

$$\ln\left(\varepsilon * - \frac{F_o}{\rho_l E}\right) = b\left[\ln\left(\frac{a}{\rho_l}\right) + \left(\frac{F_o}{\rho_l}\right)\right] \tag{15}$$

An explicit analytic expression for the creep deformation can be obtained using (5) and (9). Using these equations it is possible to obtain

$$\dot{\varepsilon}_v = \frac{K}{(1-D)}\left[\exp(\frac{NF_o}{\rho_l}) - 1)\right] \Rightarrow$$

$$\dot{\varepsilon}_v = \underbrace{K\left[\exp(N\sigma_o) - 1)\right]}_{\dot{\varepsilon}^s}\left(1 - \frac{t}{t_r}\right)^{-\left(\frac{1}{R+1}\right)} = \dot{\varepsilon}^s\left(1 - \frac{t}{t_r}\right)^{\underbrace{-\left(\frac{1}{R+1}\right)}_{\beta}}$$

with $\varepsilon_v(t=0) = \varepsilon*$. Hence

$$\int_{\varepsilon*}^{\varepsilon_v} d\varepsilon_v = \int_0^t \dot{\varepsilon}^s\left(1 - \frac{t}{t_r}\right)^{-\beta} dt \Rightarrow \varepsilon_v - \varepsilon* = \left(\tfrac{\dot{\varepsilon}^s t_r}{1-\beta}\right)\left[1 - \left(1 - \frac{t}{t_r}\right)^{(1-\beta)}\right] \Rightarrow$$

$$\varepsilon_v = \left(\tfrac{K[\exp(N\sigma_o)-1)]t_r}{1-\beta}\right)\left[1 - \left(1 - \frac{t}{t_r}\right)^{(1-\beta)}\right] + \varepsilon*$$

Finally, using (4), the following expression is obtained:

$$\varepsilon = \frac{F_o}{(1-D)\rho_l E} + \varepsilon_v \Rightarrow$$

$$\varepsilon = \frac{F_o}{\rho_l E}\left(1 - \frac{t}{t_r}\right)^{-\beta} + \left(\frac{K\left[\exp(\frac{NF_o}{\rho_l}) - 1)\right]t_r}{1-\beta}\right)\left[1 - \left(1 - \frac{t}{t_r}\right)^{(1-\beta)}\right] + \frac{F_o}{\rho_l E} + \left(\frac{aF_o}{\rho_l}\right)^b \tag{16}$$

3.3 Comparison with experimental results

In order to investigate the adequacy of the model presented here, samples of HMPE multi filaments were tested and the experimental results were checked with the model. The model parameters identified experimentally at room temperature are presented in Table 4

Table 4: Model parameters (HMPE at room temperature).

$\rho_l E$**[N]**	R **[sec]**	(S/ρ_l) **[N^{-1}]**	K **[sec^{-1}]**	(N/ρ_l) **[N^{-1}]**	(a/ρ_l) **[N^{-1}]**	b
165	10,314	$8{,}47 \times 10^{-4}$	$4{,}5 \times 10^{-7}$	$1{,}76 \times 10^{-2}$	$8{,}36 \times 10^{-4}$	0,26

The model prediction of secondary creep rate $\dot{\varepsilon}^s$ (Eq.12) for different load levels is presented in Fig. 6 and Table 5.

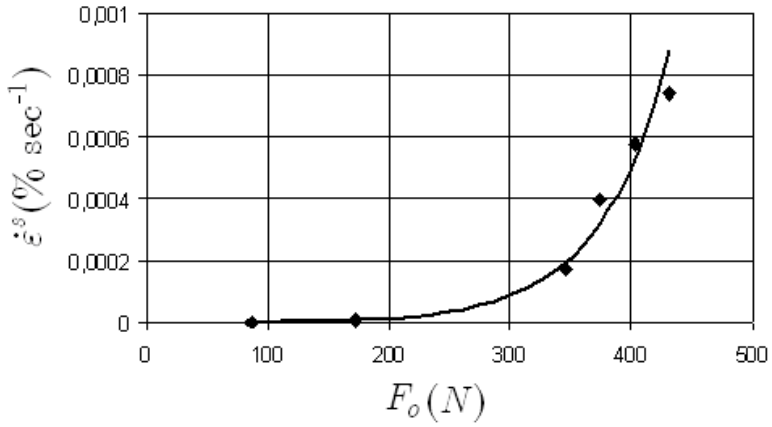

Figure 6: Secondary creep rate for different load levels. Comparison with experimental results. α = 8,3 N/sec.

Table 5: Secondary creep rate for different load levels. α = 8,3 N/sec.

F_o **(N)**	$\dot{\varepsilon}^s$ **(% sec^{-1}) experimental**	$\dot{\varepsilon}^s$ **(% sec^{-1}) model**
86,3	0,0000014	0,0000016
172,6	0,000094	0,0000089
345,3	0,00017	0,00019
374,0	0,00039	0,00032
402,7	0,00058	0,00053
431,5	0,00074	0,00088

The predicted values $\varepsilon*$ of the deformation at the beginning of the creep test using Eq. 14 is presented in Fig. 7 and Table 6.

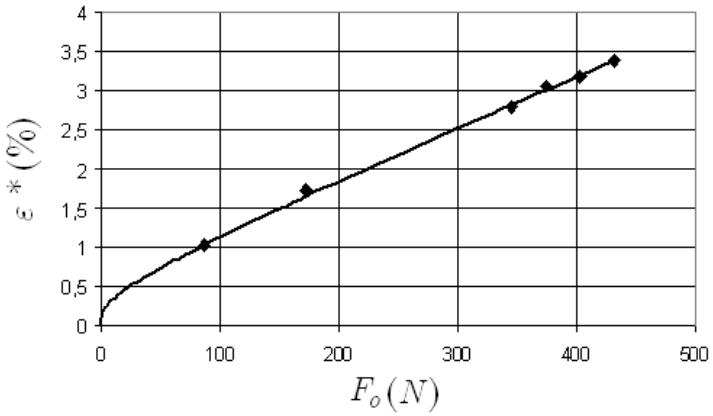

Figure 7: $\varepsilon*$ for different load levels. Comparison with experimental results.

Table 6: $\varepsilon*$ for different load levels.

F_o **(N)**	$\varepsilon*$ **(%) experimental**	$\varepsilon*$ **(%) Model**
86,3	1,02	1,02
172,6	1,73	1,64
345,3	2,79	2,80
374,0	3,05	3,00
402,7	3,18	3,18
431,5	3,37	3,38

The predicted creep lifetimes for different load levels using Eq. (9) are presented in Table 7 and Fig. 8.

Finally, Fig. 9 shows the theoretical and experimental creep curves at different load levels. The model prediction of the fracture time and elongation before rupture are in good agreement with the experimental results.

The initial stages of the creep curves are dependent on the loading history (stress and strain rates) adopted to reach the constant "initial" load F_o. Nevertheless, the final stages of the elongation-time curves (secondary and tertiary creep) seem to be little affected by this previous loading history.

Table 7: Creep lifetimes for different load levels.

F_o **(N)**	t_r **(sec) experimental**	t_r **(sec) model**
345,3	28710	28346
374,0	12162	12441
402,7	5425	5803
431,5	2935	2846

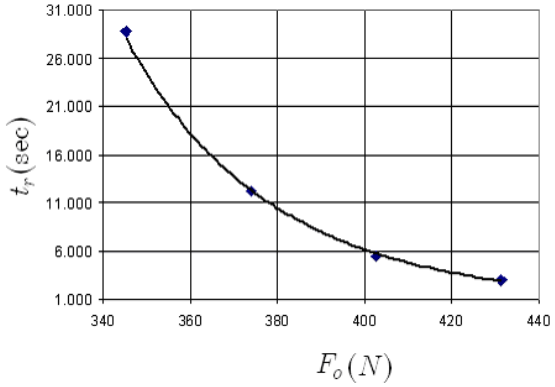

Figure 8: Creep lifetimes for different load levels. Comparison with experimental results.

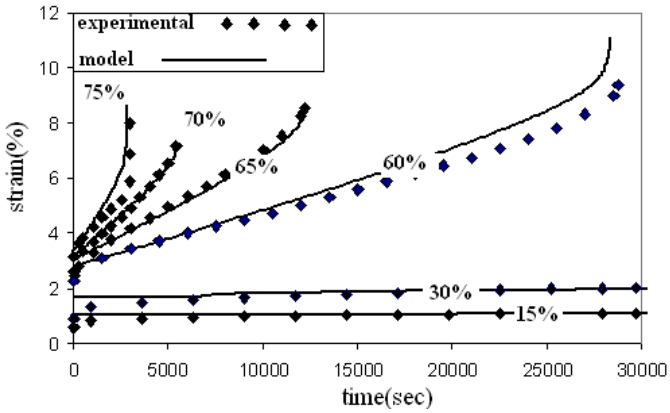

Figure 9: Creep curves at different load levels. Comparison with experimental results.

4 Conclusions

The proposed model equations combine enough mathematical simplicity to allow their usage in engineering problems with the capability to perform a physically realistic description of inelastic deformation, strain hardening, strain softening, strain rate sensitivity and damage observed in creep tests performed in HMPE multi filaments at different load levels. The main idea is to use the model to obtain the maximum information about macroscopic properties of HMPE yarns from a minimum set of laboratory tests. Only two creep tests are required to identify all the other material constants (two different load levels). The agreement between theory and experiment is very good in tests performed at 15%, 30%, 60%, 65%, 70% and 75% of the rupture load.

The present paper is a step towards the modelling of creep tests in HMPE ropes using Continuum Damage Mechanics. The analysis of creep behaviour of mooring lines accounting for the different rope constructions can be extremely complex. The mechanisms proposed so far to explain the damage initiation and propagation processes are not able to elucidate all aspects of the phenomenon in different geometry/material systems. However, in normal operation conditions, the tensile load in synthetic mooring ropes should be less than 15% of the MBL (minimum break load). For a storm condition, the maximum solicitation of a mooring line should not exceed 30% of MBL. Since the loads levels are not high in operation, it may be possible to adapt the proposed theory for yarns to ropes with complex geometric arrangements. In this case, the parameters E, K, N, S, R, a, b that appear in the theory would be geometry dependent to account for different possible sub-ropes arrangements. Heating and internal abrasion certainly reduce the lifetime but can be accounted in a thermodynamic framework. However, it is important to remark that further experimental work with HMPE ropes is still required in order to fully characterize the dependency of the parameters on the geometry.

References

[1] API-RP, *Recommended Practice for Design, Manufacture, Installation, and Maintenance of Synthetic Fiber Ropes for Offshore Mooring*, 2001.

[2] Bosman, R. & Cloos, P.J., Mooring with synthetic fiber ropes possible in all water depths. *DSM, 2003, High Performance Fibers BV – C. Design*, Offshore: Netherlands, p. 98, 1998.

[3] Schmidt, T.M., Bianchini, C., Forte, M.M.C., Amico, S.C., Voronoff, A. & Gonçalves, R.C.F., Socketing of polyester fibre ropes with epoxy resins for deep-water mooring applications. *Polymer Testing*, **25**, pp. 1044–1051, 2006.

[4] Pellegrin, I., Manmade fiber ropes in deepwater mooring applications. *Offshore Technology Conference*, Houston, pp. 1–9, 1999. OTC 10907.

[5] Sloan, F., Synthetics – the future for offshore platform moorings. *Sea Technol*, **40(4)**, p. 49, 1999.

[6] Hooker, J.G., *Synthetic fibre ropes for ultradeep water moorings in drilling and production applications*. Technical Paper Marlow Ropes, OMT: Singapore, 2000.

[7] Pearson, N.J., *Experimental snap loading of synthetic fiber ropes, Doctoral Thesis*. Virginia Polytechnic Institute and State University: Blacksburg, 2002.

[8] Petruska, D., Geyer, J., Macon, R., Craig, M., Ran, A. & Schulz, N., Polyester mooring for the mad dog spar – design issues and other considerations. *Ocean Eng*, **32(7)**, p. 767, 2005.

[9] Silva, M.O. & Chimisso, F.E.G., Experimental creep analysis on hmpe synthetic fiber ropes for offshore mooring systems. *Proceedings of the 18TH International Congress of Mechanical Engineering*, Ouro Preto, Brazil, 2005.
[10] Sampaio, E.M., Bastian, F.L. & Costa-Mattos, H.S., A simple continuum damage model for adhesively bonded butt joints. *Mechanics Research Communications*, **31(4)**, pp. 443–449, 2004.
[11] Costa-Mattos, H.S., Bastos, N. & Gomes, J.A.P., A simple model for slow strain rate and constant load corrosion tests of austenitic stainless steel in acid aqueous solution containing sodium chloride. *Corrosion Science*, **50**, pp. 2858–2866, 2008.